Mechanistic Population Pharmacokinetic Model of Oseltamivir and Oseltamivir Carboxylate Accounting for Physiological Changes to Predict Exposures in Neonates and Infants

Leonid Gibiansky[1,*], Patanjali Ravva[2,7], Neil J. Parrott[3], Rajinder Bhardwaj[4], Elke Zwanziger[3], Paul Grimsey[5], Barry Clinch[6] and Stefan Sturm[3]

A mechanistic population-pharmacokinetic model was developed to predict oseltamivir exposures in neonates and infants accounting for physiological changes during the first 2 years of life. The model included data from 13 studies, comprising 436 subjects with normal renal function (317 pediatric subjects (≥ 38 weeks postmenstrual age (PMA), ≥ 13 days old) and 119 adult subjects < 40 years). Concentration–time profiles of oseltamivir and its active metabolite, oseltamivir carboxylate (OC), were characterized by a four-compartment model, with absorption described by three additional compartments. Renal maturational changes were implemented by description of OC clearance with allometric function of weight and Hill function of PMA. Clearance of OC increased with weight up to 43 kg (allometric coefficient 0.75). Half the adult OC clearance was reached at a PMA of 45.6 weeks (95% confidence interval (CI) 41.6–49.6) with a Hill coefficient of 2.35 (95% CI 1.67–3.04). The model supports the European Union/United States-approved 3 mg/kg twice-daily oseltamivir dose for infants < 1 year (PMA ≥ 38 weeks) and allows prediction of exposures in preterm neonates.

Study Highlights

WHAT IS THE CURRENT KNOWLEDGE ON THE TOPIC?

☑ Oseltamivir is metabolized in the liver to the active metabolite, oseltamivir carboxylate (OC). Published models describe the pharmacokinetics (PKs) of oseltamivir from pediatrics (> 1 year) to geriatrics and in infants (< 1 year), primarily with a top-down approach.

WHAT QUESTION DID THIS STUDY ADDRESS?

☑ There is a need for a model that characterizes the PK properties of oseltamivir and OC, including maturation model elements predicting exposures in infants.

WHAT DOES THE STUDY ADD TO OUR KNOWLEDGE?

☑ A mechanistic population-PK (PopPK) model was developed accounting for physiological changes occurring in the first 2 years after birth; this model can be confidently applied to extrapolate PK data to term neonates.

HOW MIGHT THIS CHANGE CLINICAL PHARMACOLOGY AND TRANSLATIONAL SCIENCE?

☑ The PopPK model supports the approved dose recommendation of oseltamivir 3 mg/kg twice daily in infants < 1 year (postmenstrual age ≥ 38 weeks) and allows prediction of exposures in preterm neonates.

Oseltamivir is a prodrug, which is readily absorbed from the gastrointestinal tract and metabolized to its active form, oseltamivir carboxylate (OC), via high-capacity human carboxylesterase-1 (HCE-1), located predominantly in the liver. After hydrolysis of oseltamivir, the poorly permeable active form OC is released slowly from the liver into the systemic circulation, leading to a relatively long OC plasma half-life.[1] OC is a potent, stable, and selective inhibitor of influenza A and B neuraminidase enzymes and is excreted unchanged by the kidneys via glomerular filtration and active tubular secretion by the organic anion transport (OAT) system.[1]

[1]QuantPharm LLC, North Potomac, Maryland, USA; [2]Roche Innovation Center New York, Roche Pharmaceutical Research and Early Development, New York, New York, USA; [3]Roche Innovation Center Basel, Roche Pharmaceutical Research and Early Development, Basel, Switzerland; [4]Integrated Drug Development, Certara Strategic Consulting, Parsippany, New Jersey, USA; [5]Roche Innovation Center Welwyn, Roche Pharmaceutical Research and Early Development, Welwyn Garden City, UK; [6]Roche Products Limited, Product Development, Welwyn Garden City, UK; [7]Current address: Pfizer Inc, Global Clinical Pharmacology, New York, New York, USA. *Correspondence: Leonid Gibiansky (lgibiansky@quantpharm.com)

Received October 10, 2019; accepted January 4, 2020. doi:10.1002/cpt.1791

The pharmacokinetics (PKs) of oseltamivir and OC are linear and dose-proportional over a dose range of 50–500 mg twice daily (b.i.d.) oseltamivir.[2–5] Twice-daily administration of 75 mg oseltamivir in adolescents and adults, and 2 mg/kg oseltamivir in children aged 1–12 years, led to an area under the curve from 0–12 hours ($AUC_{0\text{-}12h}$) at steady-state of ~ 3,000 hour*ng/mL.[2–5] Oseltamivir was well tolerated at doses up to and including 500 mg b.i.d. in healthy adult volunteers.[6] Gastrointestinal effects, such as nausea and vomiting, occurred more frequently, and in a dose-related fashion in healthy volunteers exposed to high unit doses (≥ 200 mg) of oseltamivir.[6]

Orally administered oseltamivir has been approved for the treatment and prophylaxis of influenza in adults and children.[7,8] The treatment of influenza includes infants from 2 weeks of age onward in the US Food and Drug Administration (FDA),[1] and from birth onward in the European Medicines Agency (EMA) summary of product characteristics.[7] However, dosing recommendations are not intended for premature infants (i.e., those < 38 weeks postmenstrual age (PMA)). Insufficient data are available for these patients and different dosing may be required due to the immaturity of physiological functions.[7]

Acosta *et al*.[8] collected data in premature infants and results suggested that an oseltamivir dose of 1 mg/kg b.i.d. produced OC exposures similar to those observed in older infants and children receiving a 3 mg/kg b.i.d. dose. To make exposure predictions for infants, including neonates, and for untested doses, consideration should be given to developmental physiological changes affecting the PKs of oseltamivir and OC. Key factors include HCE-1 levels, glomerular filtration rate (GFR), and tubular secretion. The expression of HCE-1 increases rapidly until the end of the first year of life; analysis of liver samples from three different age groups indicated that adults (≥ 18 years) expressed significantly higher HCE-1 levels than children (0–10 years) or fetuses (82–224 gestational days).[9] Furthermore, adult (≥ 18 years) liver microsomes were ~ 4 times more active than child (0–10 years) microsomes and 10 times more active than fetal (82–224 gestational days) microsomes.[9] In addition, GFR increases rapidly during the first weeks of life and rises steadily until adult values are reached at 12–18 months of age.[10] Tubular secretion is also immature at birth and reaches adult capacity during the first 1 to 2 years of life.[11]

A physiologically-based PK model (PBPK) was previously developed to describe the PK of oseltamivir and OC in neonates and infants.[12] However, simulated steady-state exposure values with this model overpredicted those reported by Acosta *et al*.,[8] thereby limiting confidence in the PBPK approach. We aimed to develop a mechanistic population-PK (PopPK) model of oseltamivir and OC accounting for developmental physiological changes taking place during the first 2 years of life and to allow exposure predictions for infants, including neonates, and for untested doses. PK properties of oseltamivir and OC, the ontogeny of HCE-1, and the impact of kidney maturation were evaluated in the model. To our knowledge, this is the most comprehensive set of pediatric PK data included in a developmental physiological model for oseltamivir. Thus, this model can be applied to extrapolate PK data to neonates, including prediction of exposures in preterm neonates, although this lies outside the oseltamivir dosing recommendations that go down to term neonates in the European Union and 2 weeks of age in the United States.

METHODS

Clinical studies and samples

Oseltamivir and OC concentration-time data following oseltamivir oral and i.v. administration to healthy subjects and patients (**Table 1**) were used to develop the PopPK model. Study designs and PK sampling times are summarized in **Supplementary Table S1**.

All studies were conducted in accordance with country regulations, International Conference on Harmonization Good Clinical Practice guidelines, and the principles of the Declaration of Helsinki. Each study protocol was approved by applicable institutional review boards/ethics committees and health authorities, and written informed consent was obtained from all participants or their representatives.

Plasma concentrations of oseltamivir and its metabolite OC were determined using validated liquid chromatography-tandem mass spectrometry methods. The lower limits of quantification for oseltamivir and OC were 1 and 10 ng/mL, respectively. The precision and accuracy of the assays, as determined from the analysis of quality control samples, were satisfactory throughout the respective studies. Intensive PK sampling (≥ 5 samples) was performed in 11 of 13 studies. A sparse PK sampling strategy was applied in study JV16284 (two samples at steady-state conditions: at 4 hours postdose and at trough) and WV15758 (two samples at steady-state conditions: at 2–4 hours postdose and at trough). In addition, in study WV15758, selected sites collected a full PK profile (~ 7 samples/patient) for 5 pediatric patients.

Software

The PopPK analysis was conducted using a nonlinear mixed-effects modeling approach, with NONMEM software version 7.3 (ICON Development Solutions, Dublin, Ireland).[13] The first-order conditional estimation with interaction option method was used for all model runs.

Model development and covariates

The PopPK structural model has been established previously (**Figure 1**).[14] This was a four-compartment model: Two compartments described oseltamivir, one compartment described OC, and one delay compartment described oseltamivir to OC conversion. The delay compartment was required to describe formation-limited PK of OC. The absorption part of the model included three first-order processes with direct (via first-pass) input in the OC compartment and two (direct and delayed) inputs in the oseltamivir compartment. Complete metabolism from oseltamivir to OC was assumed. Random effects were added to the oseltamivir absorption rate constant (k_a), oseltamivir clearance, metabolism rate, and OC clearance. Proportional and combined error models were used for oseltamivir and OC concentrations, respectively. This model was used as a starting point and was adopted to describe pediatric population data by including body weight and age dependencies of model parameters.

Specifically, oseltamivir and OC clearance and volume parameters were assumed to increase allometrically with weight at low weights (below an estimated value), and to be independent of weight at high weights (above that value), as model parameters were more or less independent of weight in adults. Allometric coefficients were estimated for all parameters, except OC clearance. For OC clearance, the allometric coefficient was fixed at 0.75, as described by Rhodin *et al*.[10] Maturation of renal OC clearance (CL_M) was described by the Hill function of PMA:[10]

$$CL_M = CL_M^{adult} * \left(\frac{WT_i}{WT_{ref}}\right)^{0.75} * \frac{PMA^{\gamma}}{\left(PMA_{50}{}^{\gamma} + PMA^{\gamma}\right)}$$

where γ is the Hill coefficient and PMA_{50} is the maturation half time. PMA was available from only three studies (CASG114, WP22849, and NP25138). For all other subjects, the PMA was computed as age

Table 1 Summary of patients, doses, and samples

Study	References	Patients, n	Median age, years (range)	Median PMA, weeks (range)	Mean weight, kg (SD)	Mean dose, mg (SD)	Mean dose, mg/kg (SD)	Route of administration
CASG114	NCT00391768	82	0.568 (0.036–1.9)	67 (38.4–136)	7.3 (2.82)	21.8 (8.2)	3.01 (0.234)	Oral
WP15517	He *et al.* 1999[2]; Massarella *et al.* 2000[28]	28	32 (19–40)	–	77.9 (8.9)	359 (378)	4.61 (4.78)	Oral
WP15525	He *et al.* 1999[2]; Massarella *et al.* 2000[28]	16	29 (21–36)	–	78.2 (11.4)	206 (182)	2.84 (2.75)	Oral
WP15648	He *et al.* 1999[2]	5	20 (18–38)	–	78.8 (5.54)	100 (0)	1.27 (0.095)	Oral
WV15758	Whitley *et al.* 2001[29]; Winther *et al.* 2010[30]	90	6 (1–12)	–	23.9 (12)	47.1 (22.3)	1.98 (0.063)	Oral
NP15826	Oo *et al.* 2001[3]	18	11 (5–16)	–	44.7 (23.8)	74.7 (23.9)	1.81 (0.293)	Oral
JV16284	Schentag *et al.* 2007[31]	18	4.5 (1–12)	–	21.5 (10.2)	42.8 (20.5)	1.99 (0.035)	Oral
PP16351	Oo *et al.* 2003[32]	24	2.5 (1–5)	–	14.8 (3.8)	37.5 (7.7)	2.6 (0.432)	Oral
WP22849	NCT00988325	65	0.364 (0.049–0.956)	57.1 (40.9–90)	6.49 (2.1)	18.4 (7.3)	2.77 (0.32)	Oral
NV25118	NCT01050257	41	27 (13–40)	–	78.1 (16.5)	154 (50.5)	2.07 (0.847)	IV
NP25138	NCT01053663	8	0.448 (0.063–0.767)	60 (40–77)	5.85 (1.57)	16.9 (5.8)	2.82 (0.362)	IV
NP25139	NCT01033734	8	4 (1–11)	–	23.6 (6.8)	63.2 (13.9)	2.74 (0.27)	IV
NP25140	NCT02717754	33	26 (18–39)	–	77 (15.8)	148 (51)	1.99 (0.726)	IV
Total		436	4 (0.036–40)	–	33.3 (31.2)	82.4 (137)	2.55 (1.52)	

PMA, postmenstrual age.

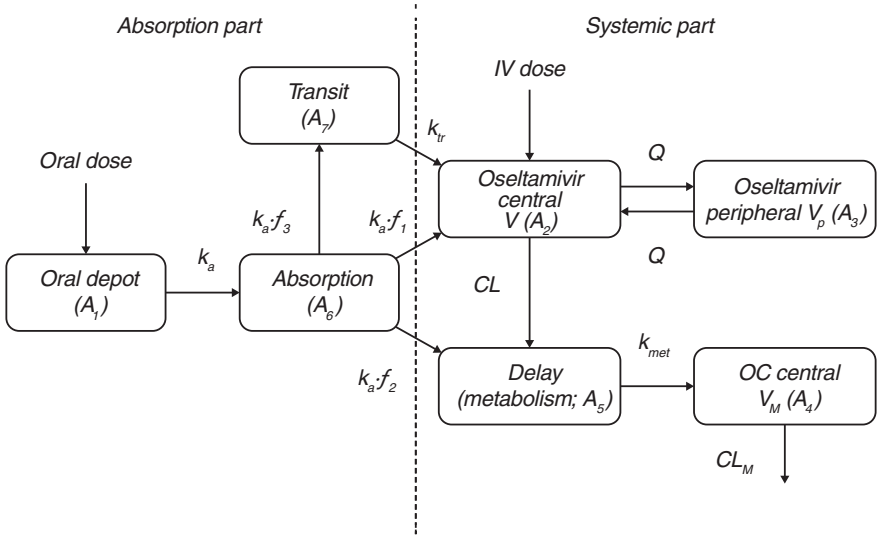

Figure 1 Schematic representation of the oseltamivir population pharmacokinetic model. Modified from Gibiansky *et al.*[14]

in weeks plus 40. Maturation of hepatic function was also tested by inclusion of age dependence for oseltamivir clearance and metabolism rate (K_{met}). Similar to renal function maturation, Hill functions of PMA were used. Model development was guided by the mechanistic considerations and diagnostic plots.

Model evaluation

Extensive evaluation of the developed model was performed. This included evaluation of diagnostic plots, visual predictive check (VPC) plots,[15] prediction-corrected VPC plots,[16] and normalized prediction distribution error (NPDE) plots.[17,18] The distributions of exposure characteristics (maximum concentration (C_{max}), minimum concentration (C_{min}), C_{median}, and C_{mean}) of the simulated data were compared with the distributions of the same characteristics in the observed dataset using exploratory graphics. Ability of the model to describe strong covariate relationships identified by the model was tested by stratifying the diagnostic plots and model evaluation procedures by the covariates of interest. Specifically, the diagnostics and VPC procedures were stratified by study.

Model-based simulations

The final PopPK model was used to estimate the individual PK parameters: Steady-state C_{max}, C_{min}, and $AUC_{0\text{-}12h}$ for oseltamivir and OC doses for all subjects. Exposure estimates were compared with exposures for adults treated with 75 mg, 150 mg, 225 mg, and 450 mg b.i.d. oseltamivir in previous clinical trials.[14] The model was also used to simulate exposure for preterm neonates following 3 mg/kg dosing regimens. Pairs and weight-postmenstrual values were taken from a database of 5,370 subjects from birth to 1 year of age[19]; these pairs were replicated 100 times.

RESULTS

Concentrations and demographics

The dataset contained 3,100 oseltamivir and 3,560 OC quantifiable plasma concentrations from 436 subjects with normal renal function enrolled in 13 studies in which oseltamivir was administered orally (n = 346; 79.4%) or i.v. (n = 90; 20.6%; **Table 1**). Most participants were pediatric subjects (n = 317; 72.7%); the remaining participants were adults < 40 years of age (n = 119; 27.3%). Overall, 265 male (60.8%) and 171 female (39.2%) subjects were included in the analysis with a wide range of weight (2.9–128 kg) and postnatal ages (13 days to 40 years). For infants (< 1 year of age) from studies CASG114, WP22489, and NP25138, PMA ranged from 38.4–90 weeks.

Model development and covariates

Preliminary investigation revealed that adult subjects had faster absorption compared with pediatric subjects. Thus, the effect of age (adults vs. pediatrics) on absorption rate constant k_a was included in the model. Subjects from study NP15826 (all aged 5–16 years) also had faster absorption than pediatric subjects from other studies. Thus, the study NP15826 effect on k_a was included in the model. Reasons for absorption differences are not known. Further, oseltamivir and OC clearance for patients from i.v. studies NP25138 and NP25139 was allowed to be lower, as these studies enrolled critically ill hospitalized children with notable comorbidities. A model with maturation of hepatic function was tested and rejected, as it did not improve the fit. The NONMEM code of the model is presented in the **Supplementary Information**.

The diagnostic plots of the final model did not reveal any deficiencies, indicating that the model provides an adequate description of oseltamivir and OC PK in subjects with normal renal function from birth up to 40 years of age. There was good concordance between the observed OC concentrations and both the population mean predicted and individual *post hoc* predicted OC concentrations across all subjects (**Figure 2**). There were no trends in the plots of the random effects vs. weight, age, PMA, sex, or creatinine clearance (**Supplementary Figure S1**). NPDE plots confirmed the ability of the model to predict both the central tendency and variability of the oseltamivir and OC concentrations. The VPC plots and NPDE plots for all studies did not indicate any systemic bias (**Supplementary Figures S2–S6**).

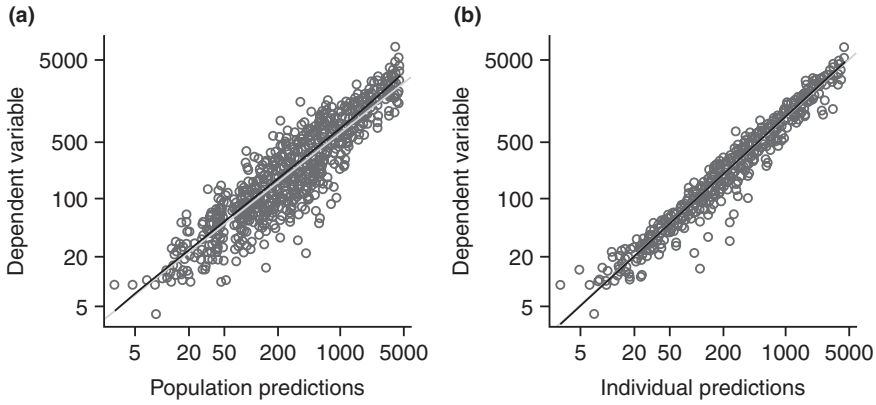

Figure 2 Relationship between observed and population mean predicted (**a**) and individual *post hoc* predicted (**b**) plasma oseltamivir carboxylate concentrations using the final population pharmacokinetic model. Pale gray solid lines represent the lines of identity and dark gray lines represent the loess (local regression smoother) trend lines.

Final PopPK model

The estimates of structural parameters and covariate effects of the final PopPK model are shown in **Table 2**. Systemic PK of oseltamivir was described by two compartments of the model; the estimates (relative standard error (RSE) %) of clearance, central volume, intercompartment clearance, and peripheral volume for a typical subject (weight ≥ 43 kg) were 197 L/hour (4.6%), 20.6 L (7.7%), 83.2 L/hour (4.1%), and 131 L (3.1%), respectively. Systemic PK of OC was described by one compartment, with clearance and volume estimates (RSE%) of 27.4 L/hour (3.6%) and 6.31 L (3.4%), respectively. Oseltamivir metabolism was described by the delay compartment with a metabolism rate constant (RSE%) of 0.0941 h^{-1} (2.3%). Oral absorption was described by three additional compartments. The oseltamivir oral dose (administered to the depot compartment) was divided (with the fractions of f1 = 0.298, f2 = 0.628, and f3 = 0.074, respectively) into three parts that were directed (via the intermediate absorption compartment) to the oseltamivir central compartment, oseltamivir metabolism compartment, and the oseltamivir delay compartment, respectively. From the oseltamivir delay compartment, oseltamivir was absorbed into the central compartment with a rate (RSE%) of 0.0515 h^{-1} (6.3%). The estimate (RSE%) of the absorption rate constant was 0.861 h^{-1} (2.7%) for subjects aged < 18 years and 71% higher (RSE 7.1%) for subjects aged > 18 years. OC PK were formation-limited, and, therefore, peripheral compartments were not identifiable in the absence of data following i.v. administration. The parameters of renal maturation were estimated as time to 50% maturation of PMA of 45.6 weeks (95% confidence interval (CI) 41.6–49.6) and the Hill coefficient of 2.35 (95% CI 1.67–3.04), which were close to the values reported by Rhodin *et al.* (PMA_{50} 47.7 weeks, Hill coefficient 3.40).[10]

Oseltamivir clearance, central volume, intercompartment clearance, peripheral volume, and metabolism rate increased with weight, with the power coefficients (RSE%) of 1.03 (3.2%), 0.65 (13.2%), 1.58 (4.7%), and 1.95 (5.8%), respectively (**Table 2**). OC clearance and central volume increased with weight, with the power coefficients (RSE%) of 0.75 (fixed), and 1.44 (7.9%), respectively. The parameters increased with weight up to 43 kg (4.2%) and were independent of weight for heavier subjects. Sex had no influence on model parameters.

The intersubject variability of oseltamivir absorption rate, oseltamivir clearance, metabolism rate, and OC clearance was moderate, in the range 30.4–34.5%, and shrinkage of these random effects was low, estimated at 17.5%, 11.9%, 26.0%, and 3.9%, respectively. The residual variability of oseltamivir concentrations was high (45.4%), whereas the residual variability of OC concentrations was low (16.2%). Models that included hepatic maturation function were tested, but were not found to be better than the final model, indicating that dependencies of oseltamivir clearance and metabolism rate on weight fully describe developmental changes of hepatic function in the pediatric population.

Oseltamivir and OC exposures

Predicted median (90% CI) oseltamivir and OC exposure metrics (AUC_{0-12h}, C_{max}, and C_{min}) at steady-state are presented by age group (postnatal age) up to 1 year following a 3 mg/kg b.i.d. oral dosing regimen of oseltamivir (**Table 3**). **Figure 3** shows the predicted steady-state OC AUC_{0-12h} by age group, which were compared with previous clinical trial data in adults receiving oral conventional b.i.d. doses of oseltamivir (75 mg, 150 mg, 225 mg, and 450 mg). Exposures of oseltamivir were similar across the different age groups, whereas exposure metrics of OC increased with decreasing age. In the youngest age group of 0–1 month, the median predicted AUC_{0-12h} of OC was ~ 40% higher than in infants aged 9–12 months. Furthermore, exposure metrics were very variable in the youngest age group, and the predicted 90% CI covered the entire range of the predicted 90% CI of all other age groups up to 1 year.

The developed mechanistic PopPK model predicted exposures of oseltamivir and OC as a function of PMA in the range 22–90 weeks following a 3 mg/kg b.i.d. oral dosing regimen of oseltamivir. Oseltamivir exposure metrics remained unchanged across the entire PMA range (**Figure 4**), whereas exposure metrics of OC increased for decreasing ages, which is consistent with postnatal age.

DISCUSSION

The aim of this modeling work was to describe the PK properties of oseltamivir (including formation rate kinetics of OC)

Table 2 Estimates of structural parameters and covariate effects for the final population PK model including interindividual variability parameters and residual model parameters

Parameter			Value	%RSE	95% CI	Variability	Shrinkage
Structural model parameters							
CL (L/hour)	θ_1	Oseltamivir clearance	197	4.62	180–215		
V_C (L)	θ_2	Oseltamivir central volume	20.6	7.74	17.5–23.7		
Q (L/hour)	θ_3	Oseltamivir intercompartment clearance	83.2	4.12	76.5–89.9		
V_P (L)	θ_4	Oseltamivir peripheral volume	131	3.11	123–139		
CL_M (L/hour)	θ_5	OC clearance	27.4	3.58	25.4–29.3		
V_M (L)	θ_6	OC volume	6.31	3.37	5.89–6.73		
k_{met} (1/hour)	θ_7	Oseltamivir to OC metabolism rate	0.0941	2.32	0.0898–0.0984		
k_a (1/hour)	θ_8	Absorption rate constant	0.861	2.73	0.815–0.907		
FF_2 [a]	θ_9	Fraction parameter[a]	2.11	7.19	1.81–2.41		
FF_3 [a]	θ_{10}	Fraction parameter[a]	0.251	2.1	0.24–0.261		
k_{tr} (1/hour)	θ_{11}	Transit compartment rate constant	0.0515	6.25	0.0452–0.0578		
AGE_{50}	θ_{12}	50% maturation of PMA	45.6	4.48	41.6–49.6		
γ	θ_{13}	Hill coefficient	2.35	14.9	1.67–3.04		
Covariate effect parameters							
$CL_{25138,25139}$	θ_{14}	Effect of study NP25138 and NP25139 on oseltamivir clearance	0.488	14	0.354–0.622		
$CL_{M,\ 25138,25139}$	θ_{15}	Effect of study NP25138 and NP25139 on OC clearance	0.49	9.4	0.4–0.58		
$k_{a,AGE\geq18}$	θ_{16}	Absorption rate for age ≥ 18 years	1.71	7.05	1.47–1.95		
CL_{WT}	θ_{17}	Power of weight on oseltamivir clearance	1.03	3.15	0.967–1.09		
$V_{C,WT}$	θ_{18}	Power of weight on oseltamivir central volume	0.65	13.2	0.481–0.819		
Q_{WT}	θ_{19}	Power of Q on weight	1.95	5.81	1.73–2.17		
$V_{P,WT}$	θ_{20}	Power of weight on oseltamivir peripheral volume	1.58	4.69	1.44–1.73		
$CL_{M,WT}$	θ_{21}	Power of weight on OC clearance	0.75	Fixed			
$V_{M,WT}$	θ_{22}	Power of weight on OC volume	1.44	7.87	1.22–1.67		
$k_{a,15826}$	θ_{23}	Effect of study NP15826 on absorption rate	1.7	14.8	1.21–2.2		
WT_{ref}	θ_{24}	Reference weight	43.0	4.15			
Interindividual variability parameters							
ω^2_{CL}	$\Omega(1,1)$	Variance of oseltamivir clearance	0.119	7.14	0.103–0.136	CV 34.5%	11.9%
ω^2_{CLM}	$\Omega(2,2)$	Variance of OC clearance	0.118	5.83	0.105–0.132	CV 34.4%	3.9%
ω^2_{kmet}	$\Omega(3,3)$	Variance of oseltamivir to OC metabolism rate	0.0922	12.4	0.0697–0.115	CV 30.4%	26.0%
ω^2_{ka}	$\Omega(4,4)$	Variance of absorption rate constant	0.116	12.9	0.087–0.146	CV 34.1%	17.5%

(Continued)

Table 2 (Continued)

Parameter			Value	%RSE	95% CI	Variability	Shrinkage
Residual model parameters							
$\sigma^2_{O,prop}$	Σ(1,1)	Oseltamivir proportional error	0.206	1.96	0.198–0.214	CV 45.4%	5.7%
$\sigma^2_{OC,prop}$	Σ(2,2)	OC proportional error	0.0264	1.17	0.0258–0.027	CV 16.2%	10.4%
$\sigma^2_{OC,add}$	Σ(3,3)	OC additive error	25.4	22.2	14.3–36.4	SD 5.04	

CI, confidence interval; CV, coefficient of variation; OC, oseltamivir carboxylate; PK, pharmacokinetic; PMA, postmenstrual age; RSE, relative standard error (standard error/parameter estimate).
[a]$f_1 = 1/(1 + FF_2 + FF_3)$, fraction of dose that enters oseltamivir compartment directly; $f_2 = FF_2/(1 + FF_2 + FF_3)$, fraction of dose that enters metabolism compartment; $f_3 = FF_3/(1 + FF_2 + FF_3)$ fraction of dose that enters oseltamivir compartment with delay (transit compartment).

Table 3 Predicted median (90% CI) of oseltamivir and oseltamivir carboxylate exposure by age group following a 3 mg/kg b.i.d. oral dosing regimen of oseltamivir

		Oseltamivir			Oseltamivir carboxylate		
Age, months	Patients, *n*	AUC, ng/mL*hour	C_{max}, ng/mL	C_{min}, ng/mL	AUC, ng/mL*hour	C_{max}, ng/mL	C_{min}, ng/mL
0–1	13	215 (131–325)	55.5 (3.8–91.1)	3.33 (1.93–5.14)	6,240 (1,410–9,510)	664 (142–985)	362 (86.2–576)
1–3	33	227 (137–365)	66.4 (32.2–96.3)	3.41 (1.86–6.5)	5,280 (3,650–8,200)	583 (378–850)	302 (187–486)
3–6	25	240 (166–377)	68.6 (38.6–97.5)	3.82 (2.3–6.43)	4,570 (3,090–6,860)	498 (322–746)	288 (173–426)
6–9	35	302 (190–439)	74.7 (46.6–125)	4.72 (2.83–7.45)	4,310 (2,830–6,820)	459 (284–701)	257 (169–404)
9–12	44	273 (175–407)	67.1 (41.5–116)	4.62 (2.6–7.87)	4,500 (1,900–6,470)	453 (197–675)	264 (115–391)

AUC, area under the curve; CI, confidence interval; C_{max}, maximum concentration; C_{min}, minimum concentration.

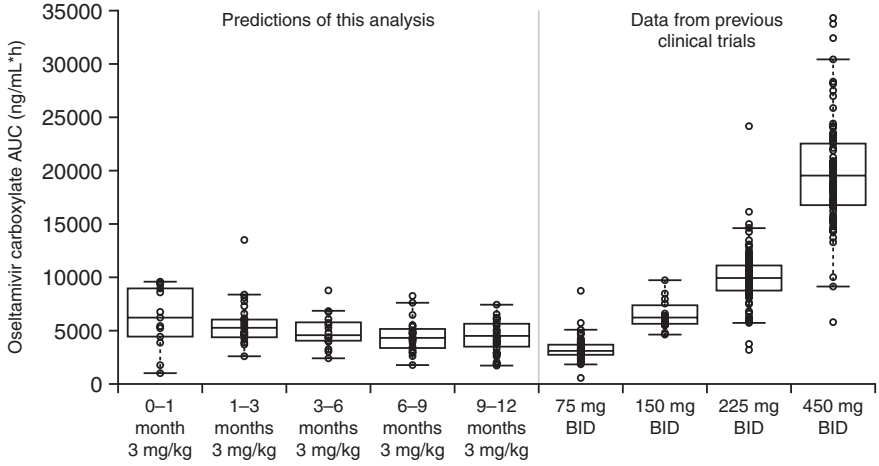

Figure 3 Comparison of predicted steady-state oseltamivir carboxylate area under the curve from 0 to 12 hours (AUC_{0-12h}) following oral twice-daily (b.i.d.) dosing. The values are plotted by groups using box and whisker plots. Median values for each group are designated by a black line in the center of the box. Boxes indicate the interquartile range (IQR). Whiskers represent 1.5*IQR. Individual values are marked by circles.

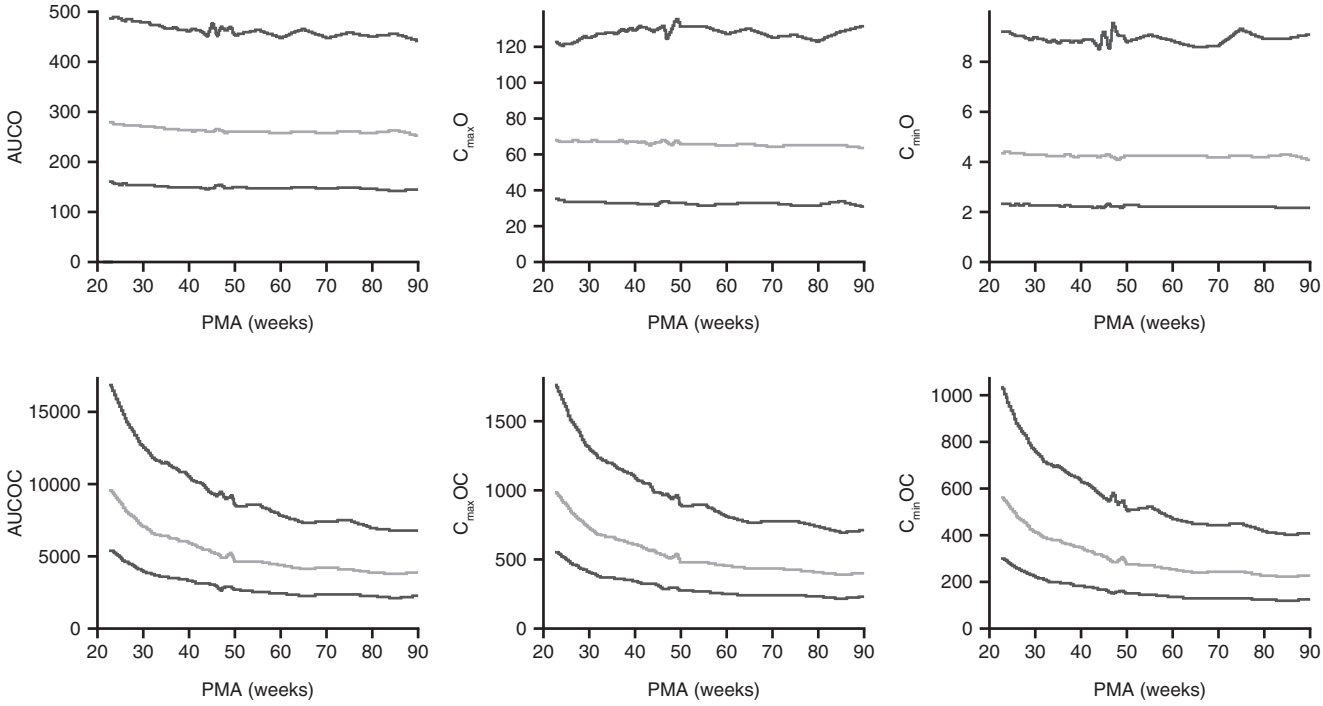

Figure 4 Dependence of predicted steady-state oseltamivir (O; top row) and oseltamivir carboxylate (OC; bottom row) exposure metrics (area under the curve from 0 to 12 hours (AUC_{0-12h}), maximum plasma concentation (C_{max}), minimum plasma concentration (C_{min})) on postmenstrual age (PMA) following 3 mg/kg oral twice-daily dosing (median and 90% prediction intervals).

administered to subjects from birth to 40 years old, to describe developmental physiological changes taking place during the first 2 years of life, and to identify the covariates that influence oseltamivir PK in the target population. All available PK data from 317 pediatric patients enrolled in 13 studies were included in the dataset, together with data from 119 young adults (aged 18–40 years) with normal renal function (creatinine clearance ≥ 90 mL/minutes/1.73 m^2).

Different PopPK models have been developed previously.[14,20–23] The same structural model as applied to adult patients with and without renal impairment was used,[14] as it accounts for physiological aspects of the PK of oseltamivir. The absorption part of the model includes three first-order processes and a compartment that describes the oseltamivir to OC conversion. From this compartment, representing the liver, OC is relatively slowly released into the systemic circulation leading to a prolonged half-life (flip-flop kinetics). This model was modified to address maturational changes.

The metabolism of oseltamivir to OC is mediated via the HCE-1 enzyme, located predominantly in the liver and at low levels in the intestine.[24] A surge occurs in the expression

of HCE-1 during the postneonatal stage, such that the hydrolytic capacity of HCE-1 is gained rapidly after birth.[25] Age-dependent hydrolysis via the HCE-1 enzyme could in theory affect exposure to oseltamivir and OC, especially in very young infants. Based on PBPK modeling, it is suggested that levels of esterase activity in newborns are sufficient for conversion of oseltamivir into OC, with OC levels relatively insensitive to changes in hydrolysis via HCE-1.[12] Consistent with these findings, attempts to include hepatic maturation (i.e., by increasing the clearance of oseltamivir with PMA) did not improve the fit of the model, which indicates that HCE-1 activity in newborns does not have a major impact on the extent and rate of conversion of oseltamivir into OC. Thus, hepatic maturation was not incorporated into the model.

OC is not metabolized, but is excreted in urine without further change. Renal clearance of OC exceeds the GFR indicating that renal tubular secretion contributes to the elimination of the compound. Renal tubular secretion of OC occurs via the OAT system.[1] The GFR increases rapidly during the first weeks of life and then rises steadily until adult values are reached at 12–18 months of age.[10] Similarly, tubular secretion is immature at birth and reaches adult capacity during the first 1–2 years of life.[11] Changes in active tubular secretion (e.g., OAT) were described by changes in GFR. This is based on the observation that the curve of para-aminohippuric acid clearance (which is secreted primarily via OAT[1] and only 20–30% is filtered[26]), is parallel to the curve for changes in GFR during postnatal development.[11]

Renal maturation function was described by a sigmoid hyperbolic model (Hill function) that had a major effect on clearance of OC and, therefore, on OC exposure. PMA was used to describe the nonlinear increase in GFR from very premature neonates to young adults, as PMA has been shown to be a better descriptor of maturational changes than postnatal age.[10] PMA that corresponds to 50% maturation of the GFR was estimated to be 45.6 weeks, which is consistent with the 47.7 weeks reported by Rhodin *et al*.[10]

Dependencies of all parameters on weight and renal maturation of OC clearance were included in the model. All model parameters were well estimated, and diagnostic plots and various model evaluation simulations (including VPC procedures) indicated the ability of the model to predict the central tendency and the spread of oseltamivir and OC concentrations in all age groups.

Predicted exposure metrics of oseltamivir remained unchanged across the PMA range from 22–90 weeks. This is consistent with data from the literature, which showed that, even in premature babies, oseltamivir concentrations were comparable to those in older children (based on a mg/kg dosing regimen).[8]

For the active metabolite, the exposure metrics of OC increased with decreasing age. In the lowest age group of 0–1 month, the predicted median exposures ($AUC_{0\text{-}12h}$) of OC at steady-state were ~ 40% higher than in infants aged 9–12 months. However, the exposure was very variable in the lowest age group. Thus, the slightly higher OC AUCs for younger infants safeguards from underexposure and subsequent risk of treatment failure. This modest increase in OC exposure is not considered to alter the safety and tolerability of oseltamivir due to its broad safety window. These PopPK results reinforce the recommendations for infants in both the United States and European Union labels. In addition, it may allow extrapolation of PK data to infants with a PMA of 34 to 38 weeks.

Within the analyzed dataset, no observed PK data were available below a PMA of 38 weeks, and there was only one patient with a postnatal age < 2 weeks. Based on predictions of this mechanistic PopPK model, an oseltamivir dose of 2 mg/kg b.i.d. for infants with a PMA of 34 to 38 weeks may be appropriate, taking a higher variability into account while safeguarding these patients from underexposure. Extrapolation to patients with a PMA below 34 weeks should be avoided, or made with caution, as nephrogenesis has just completed by this age.[27]

In conclusion, the developed PopPK model, accounting for physiological changes taking place in the first 2 years after birth, can be applied to extrapolate PK data to term neonates. As such, the developed model supports the approved dose recommendation of 3 mg/kg b.i.d. for oseltamivir in infants < 1 year of age (with a PMA ≥ 38 weeks). In addition, it may allow prediction of exposures in preterm neonates, although use of oseltamivir in these patients lies outside the labeled oseltamivir dosing recommendations that go down to term neonates in the European Union and 2 weeks of age in the United States.

SUPPORTING INFORMATION

Supplementary information accompanies this paper on the *Clinical Pharmacology & Therapeutics* website (www.cpt-journal.com).

Table S1. Summary of clinical studies used in the model building.
Figure S1. Relationships of the interindividual random effects with (**A**) weight, (**B**) age, (**C**) postmenstrual age (PMA), (**D**) creatinine clearance, and (**E**) gender for the final model.
Figure S2. Prediction-corrected visual predictive check for the final model: Concentrations of oseltamivir versus nominal time after dose administration for all subjects.
Figure S3. Prediction-corrected visual predictive check for the final model: Concentrations of oseltamivir carboxylate versus nominal time after dose administration for all subjects.
Figure S4. Prediction-corrected visual predictive check for the final model: Concentrations of oseltamivir and oseltamivir carboxylate versus nominal time after dose administration for subjects under 1 year old.
Figure S5. Normalized prediction distribution errors (NPDE) plots for the final model for oseltamivir.
Figure S6. Normalized prediction distribution errors (NPDE) plots for the final model for oseltamivir carboxylate.
NONMEM code for the final PK model.

ACKNOWLEDGMENTS

Third-party medical writing support, under the direction of the authors, was provided by Fiona Fernando, PhD, of Gardiner-Caldwell Communications, and was funded by F. Hoffmann-La Roche Ltd.

FUNDING

The CASG114 study was supported by National Institutes of Health funding from the Division of Microbiology and Infectious Diseases, National Institute of Allergy and Infectious Diseases (contracts N01-AI-30025, N01-AI-65306, N01-AI-15113, and N01-AI-62554). All other studies were sponsored by F. Hoffmann-La Roche Ltd.

CONFLICT OF INTEREST

L.G. and R.B. are paid consultants for Roche Ltd. P.R. is a former employee of Roche and holds stocks at F. Hoffmann-La Roche. E.Z. is a Roche employee. N.J.P., P.G., B.C., and S.S. are Roche employees and hold stocks at F. Hoffmann-La Roche.

AUTHOR CONTRIBUTIONS

L.G. and S.S. wrote the manuscript. L.G., P.R., N.J.P., R.B., B.C., and S.S. designed the research. L.G., P.R., R.B., E.Z., P.G., B.C., and S.S. performed the research. L.G., P.R., E.Z., and P.G. analyzed the data.

DATA SHARING STATEMENT

Qualified researchers may request access to individual patient level data through the clinical study data request platform (www.clinicalstudydatarequest.com). Further details on Roche's criteria for eligible studies are available at https://clinicalstudydatarequest.com/Study-Sponsors/Study-Sponsors-Roche.aspx and details on Roche's Global Policy on Sharing of Clinical Information and how to request access to related clinical study documents are available at https://www.roche.com/research_and_development/who_we_are_how_we_work/clinical_trials/our_commitment_to_data_sharing.htm.

1. Food and Drug Administration. Oseltamivir package insert <http://www.fda.gov/downloads/Drugs/DrugSafety/DrugShortages/UCM183850.pdf>. Accessed August 15, 2019.
2. He, G. *et al.* Clinical pharmacokinetics of the prodrug oseltamivir and its active metabolite Ro 64–0802. *Clin. Pharmacokinet.* **37**, 471–484 (1999).
3. Oo, C. *et al*. Pharmacokinetics and dosage recommendations for an oseltamivir oral suspension for the treatment of influenza in children. *Paediatr. Drugs* **3**, 229–236 (2001).
4. Treanor, J.J. *et al*. Efficacy and safety of the oral neuraminidase inhibitor oseltamivir in treating acute influenza: a randomized controlled trial. US Oral Neuraminidase Study Group. *JAMA* **283**, 1016–1024 (2000).
5. Nicholson, K.G. *et al*. Efficacy and safety of oseltamivir in treatment of acute influenza: a randomised controlled trial. Neuraminidase Inhibitor Flu Treatment Investigator Group. *Lancet* **355**, 1845–1850 (2000).
6. Dutkowski, R. *et al*. Safety and pharmacokinetics of oseltamivir at standard and high dosages. *Int. J. Antimicrob. Agents* **35**, 461–467 (2010).
7. Tamiflu® (oseltamivir phosphate) summary of product characteristics. Roche <http://www.mhra.gov.uk/home/groups/comms-ic/documents/websiteresources/con046637.pdf>. Accessed August 15, 2019.
8. Acosta, E.P. *et al*. Oseltamivir dosing for influenza infection in premature neonates. *J. Infect. Dis.* **202**, 563–566 (2010).
9. Yang, D. *et al*. Human carboxylesterases HCE1 and HCE2: ontogenic expression, inter-individual variability and differential hydrolysis of oseltamivir, aspirin, deltamethrin and permethrin. *Biochem. Pharmacol.* **77**, 238–247 (2009).
10. Rhodin, M.M. *et al*. Human renal function maturation: a quantitative description using weight and postmenstrual age. *Pediatr. Nephrol.* **24**, 67–76 (2009).
11. Kearns, G.L. *et al*. Developmental pharmacology – drug disposition, action, and therapy in infants and children. *N. Engl. J. Med.* **349**, 1157–1167 (2003).
12. Parrott, N. *et al*. Development of a physiologically based model for oseltamivir and simulation of pharmacokinetics in neonates and infants. *Clin. Pharmacokinet.* **50**, 613–623 (2011).
13. Beal, S. *et al*. *NONMEM User's Guides (1989–2014)* (Icon Development Solutions, Ellicott City, MD, 2014).
14. Gibiansky, L. *et al*. Population pharmacokinetic analysis of oseltamivir and oseltamivir carboxylate following intravenous and oral administration to patients with and without renal impairment. *J. Pharmacokinet. Pharmacodyn.* **42**, 225–236 (2015).
15. Yano, Y. *et al*. Evaluating pharmacokinetic/pharmacodynamic models using the posterior predictive check. *J. Pharmacokinet. Pharmacodyn.* **28**, 171–192 (2001).
16. Bergstrand, M. *et al*. Prediction-corrected visual predictive checks for diagnosing nonlinear mixed-effects models. *AAPS J.* **13**, 143–151 (2011).
17. Brendel, K. *et al*. Metrics for external model evaluation with an application to the population pharmacokinetics of gliclazide. *Pharm. Res.* **23**, 2036–2049 (2006).
18. Mentré, F. & Escolano, S. Prediction discrepancies for the evaluation of nonlinear mixed-effects models. *J. Pharmacokinet. Pharmacodyn.* **33**, 345–367 (2006).
19. Sumpter, A.L. & Holford, N.H. Predicting weight using postmenstrual age – neonates to adults. *Pediatr. Anaesth.* **21**, 309–315 (2011).
20. Kamal, M.A. *et al*. Identification of new oral dosing regimens for the neuramindase inhibitor oseltamivir in patients with moderate and severe renal impairment. *Clin. Pharmacol. Drug Dev.* **4**, 326–336 (2015).
21. Kamal, M.A. *et al*. Population pharmacokinetics of oseltamivir: pediatrics through geriatrics. *Antimicrob. Agents Chemother.* **57**, 3470–3477 (2013).
22. Rayner, C.R. *et al*. Population pharmacokinetics of oseltamivir when coadministered with probenecid. *J. Clin. Pharmacol.* **48**, 935–947 (2008).
23. Kamal, M.A. *et al*. The posology of oseltamivir in infants with influenza infection using a population pharmacokinetic approach. *Clin. Pharmacol. Ther.* **96**, 380–389 (2014).
24. Ohura, K. *et al*. Establishment and characterization of a novel caco-2 subclone with a similar low expression level of human carboxylesterase 1 to human small intestine. *Drug Metab. Dispos.* **44**, 1890–1898 (2016).
25. Shi, D. *et al*. Surge in expression of carboxylesterase 1 during the post-neonatal stage enables a rapid gain of the capacity to activate the anti-influenza prodrug oseltamivir. *J. Infect. Dis.* **203**, 937–942 (2011).
26. Tett, S.E. *et al*. Principles and clinical application of assessing alterations in renal elimination pathways. *Clin. Pharmacokinet.* **42**, 1193–1211 (2003).
27. Saint-Faust, M. *et al*. Renal development and neonatal adaptation. *Am. J. Perinatol.* **31**, 773–780 (2014).
28. Massarella, J.W. *et al*. The pharmacokinetics and tolerability of the oral neuraminidase inhibitor oseltamivir (Ro 64–0796/GS4104) in healthy adult and elderly volunteers. *J. Clin. Pharmacol.* **40**, 836–843 (2000).
29. Whitley, R.J. *et al*. Oral oseltamivir treatment of influenza in children. *Pediatr. Infect. Dis. J.* **20**, 127–133 (2001).
30. Winther, B. *et al*. Impact of oseltamivir treatment on the incidence and course of acute otitis media in children with influenza. *Int. J. Pediatr. Otorhinolaryngol.* **74**, 684–688 (2010).
31. Schentag, J.J. *et al*. Similarity in pharmacokinetics of oseltamivir and oseltamivir carboxylate in Japanese and Caucasian subjects. *J. Clin. Pharmacol.* **47**, 689–696 (2007).
32. Oo, C. *et al*. Pharmacokinetics of anti-influenza prodrug oseltamivir in children aged 1–5 years. *Eur. J. Clin. Pharmacol.* **59**, 411–415 (2003).